Enabling efficient and robust analysis of tandem repeats in genomic data using wavefront-based string decomposer

Junhai Qi, Zhidong Yang, Ting Yu, et al.

Genome Res. published online April 8, 2026
Access the most recent version at doi:10.1101/gr.281346.125

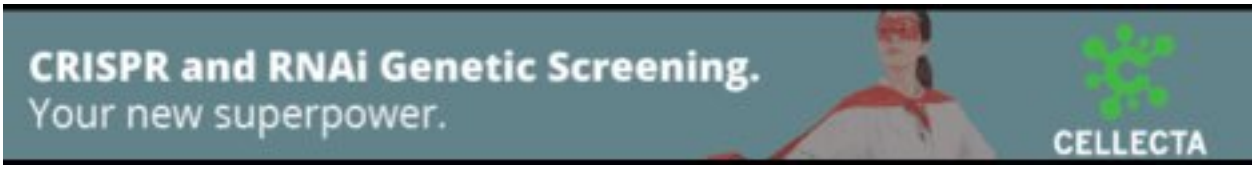

Enabling efficient and robust analysis of tandem repeats in genomic data using wavefront-based string decomposer

Junhai Qi[1], Zhidong Yang[2], Ting Yu[1, *], Guojun Li[1, *]

[1]Research Center for Mathematics and Interdisciplinary Sciences (Frontiers Science Center for Nonlinear Expectations), Shandong University, Qingdao, Shandong 266237, China; [2]Department of Chemical and Biological Engineering, The Hong Kong University of Science and Technology, Hong Kong S.A.R., China, 999077

[*]Correspondence to: tingy@sdu.edu.cn and gjli@sdu.edu.cn

Abstract

Tandem repeats (TRs) analysis is crucial for understanding genome structure and variation. However, string decomposition, a key challenge in TRs analysis, remains computationally demanding. In this study, we introduce WSD (**W**avefront-based **S**tring **D**ecomposer), a novel algorithm that enhances efficiency and accuracy in TRs decomposition. By integrating wavefront techniques, WSD significantly reduces computational and memory costs. Additionally, two adaptive strategies minimize parameter sensitivity and further improve efficiency. Through extensive experiments, we demonstrate that WSD outperforms current state-of-the-art (SOTA) methods, achieving an average speedup of ~2.33× and reducing memory usage by two orders of magnitude when analyzing human TRs.

Introduction

TRs are genomic sequences composed of tandemly arranged DNA repeat units. TRs are broadly categorized into short tandem repeats (STRs) and long tandem repeats (LTRs) based on repeat unit length. STRs typically consist of 1–6 base pair (bp) repeat units, whereas LTRs can span hundreds of base pairs. In human centromeric α-satellite regions, the core repeat unit—the monomer—is approximately 171 bp in length. Monomers can further organize into higher-order

repeats (HORs), which are repeated hundreds to thousands of times. STR expansions contribute to approximately 60 human genetic disorders (Depienne and Mandel, 2021), while LTRs are associated with diseases such as pancreatic cancer (Ting et al., 2011).

A key computational challenge in TR analysis is the string decomposition problem (decomposing TRs into repetitive units). Dvorkina et al. formally defined this problem and introduced StringDecomposer (SD) (Dvorkina et al., 2020), a computational method that models decomposition as a longest-path search in a string decomposition graph. Despite advancements, complete centromere assembly remains challenging due to the complexity of repetitive structures (Li and Durbin, 2024). Leveraging SD, CentroFlye (Bzikadze and Pevzner, 2020) was developed as a centromere-specific assembly tool, enabling the first complete reconstruction of human Chromosome 6 and X. Furthermore, string decomposition algorithms play a critical role in resolving mosaic tandem repeats (Masutani et al., 2023) and HORs (Kunyavskaya et al., 2022; Gao et al., 2023; Qi et al., 2025), facilitating large-scale comparative analyses of TR variation across human populations (Ichikawa et al., 2023; Gao et al., 2024; Logsdon et al., 2024).

The string decomposition problem is fundamentally a dynamic programming (DP) problem (see **Methods**). While analogous to sequence alignment, it exhibits higher computational complexity in both time and space, making traditional DP-based methods impractical for large-scale genomic datasets. Most sequence alignment algorithms, rely on classical Needleman-Wunsch-DP paradigms (Needleman and Wunsch, 1970). However, recent advancements in wavefront-based approaches led to the development of Wavefront Alignment (WFA) (Marco-Sola et al., 2021), which greatly improves efficiency in the global alignment of highly similar sequences. Several modern alignment tools now incorporate WFA algorithm to optimize performance (Zhang et al., 2025; Bahk and Sung, 2024).

In this study, we introduce the wavefront paradigm and present WSD, a new algorithm for fast string decomposition. By incorporating two adaptive strategies, WSD achieves markedly higher speed and lower memory consumption, while reducing the sensitivity of decomposition results to parameter settings. These improvements enable more robust, accurate, and efficient analysis of TR reads and assemblies.

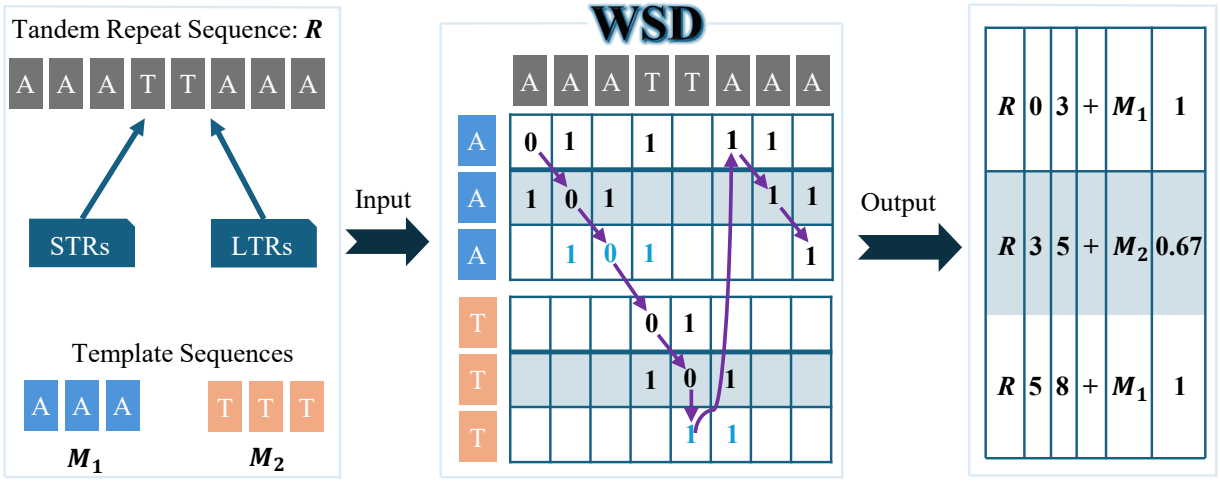

Figure 1: **Overview of WSD.** WSD constructs a DP matrix similar to sequence alignment (with mismatch and gap penalties set to 1 in this example). Each cell in the matrix represents the minimum decomposition cost at that position. The purple arrows indicate the decomposition path, analogous to an alignment path, which determines the final decomposition result. Blue-labeled DP cells represent "template-transition" cells, allowing the decomposition path to jump between specific DP cells of different templates. The WSD output is a TSV file with columns: TR name/TR start/TR end/alignment direction ("+" for forward, "-" for reverse complement)/template name/identity score.

Results

Overview of WSD

Figure 1 illustrates the workflow of the WSD algorithm. The input to the WSD algorithm consists of TRs and a set of template sequences, which can be either STRs or LTRs, while the output is a decomposition result. The decomposition comprises an ordered set of non-overlapping blocks, each representing a subsequence of the tandem repeat sequence with a defined start and end position. Each block is associated with a specific template sequence and an identity score, indicating the degree of similarity between the block and the template.

Fundamentally, WSD is a DP-based algorithm, primarily composed of the extend and expand functions (Details in **Methods**). Given a fixed cost score, the extend function attempts to extend along diagonals in the DP matrix that satisfy specific conditions until reaching the final cell. If no diagonal can reach the final cell due to an insufficient cost score, the expand function activates, enabling additional diagonals to extend. This iterative process continues until a diagonal successfully reaches the final cell.

To enhance computational efficiency, WSD employs an adaptive partitioning strategy, segmenting the tandem repeat sequence into fixed-length subsequences, individually decomposing them, and merging the results to obtain the final decomposition. Additionally, an adaptive pruning strategy is integrated to further accelerate the iterative process.

Benchmarking of WSD

There are many tools for tandem repeat analysis, such as TRF (Benson, 1999) and NCRF (Harris et al., 2019), but none of them explicitly solve the string decomposition problem, which has been extensively discussed (Dvorkina et al., 2020). TRviz (Park et al., 2023) was developed for decomposing and visualizing tandem repeat units, while vamos (Ren et al., 2023) focuses on annotating variable-number tandem repeats (VNTRs). A common subproblem in these methods is string decomposition. However, their decomposition approaches are fundamentally similar to SD (vamos uses SD directly), SD currently represents SOTA. Therefore, WSD was benchmarked exclusively against SD.

We compared WSD and SD on both simulated and real datasets. The experimental environment and command lines are provided in Supplementary Note 1. The simulated datasets include simulated assembly datasets and simulated sequencing datasets. The simulated assembly datasets were generated following the methodology of HiCAT (Gao et al., 2023), with the same simulation script parameters, resulting in 36 different types of datasets (S1-S36, see Supplemental Table S1), each containing 100 assemblies. The simulated sequencing datasets have different read lengths and error rates (SR1-SR24, see Supplemental Table S2), each dataset contains 500 reads. The generation details are provided in Supplementary Note 2. On the simulated dataset, two decomposition methods can be applied: Monomer decomposition (using monomers as templates to complete the decomposition) and HOR decomposition (using HORs as templates to complete the decomposition).

Additionally, we evaluated the algorithms on well-characterized centromeric regions from two reference genomes: the centromeres of the human CHM13-T2T genome (v2.0) (Nurk et al., 2022) and those of *Arabidopsis thaliana* (Naish et al., 2021). Given the heterogeneity of HOR organization in real centromeres, and the fact that HORs do not necessarily share a fixed number or ordering of monomers, we performed decomposition on these real datasets using monomers as the fundamental templates. This choice allows a consistent and general evaluation of algorithmic performance under realistic centromeric complexity. Centromeric region templates were obtained from HORmon (Kunyavskaya et al., 2022).

The primary evaluation metrics are the running time and memory usage. Theoretically, both algorithms are exact and should guarantee perfect decomposition across all datasets. However, to accelerate computation, TRs are often divided into a series of overlapping subsequences. The decomposition results of these subsequences are then merged to obtain the final decomposition of TRs. This approach may miss the optimal decomposition, so we also introduced

three metrics to evaluate accuracy: Bias, Decomposition Accuracy, and Decomposition Distance, defined as follows.

Both methods produce decompositions as a series of contiguous blocks, where each block has a start position and an end position on the reference, a template label, and an identity score representing its similarity to the template. We define GTN as the ground-truth number of blocks and AN as the number of blocks obtained by the algorithm. Bias is calculated as:

$$\text{Bias} = |GTN - AN| \tag{1}$$

When the bias is 0, assuming the true template label of the i-th block is TM_i and the template label obtained by the algorithm is AM_i, the decomposition accuracy is defined as:

$$\text{Accuracy} = \frac{|\{AM_i \mid \text{if } AM_i = TM_i, i = 1, 2, ..., GTN\}|}{GTN} \tag{2}$$

Since no ground-truth template labels are available for the real dataset, we cannot directly compute decomposition accuracy. Therefore, we estimate the algorithm's accuracy on real data using the Decomposition Distance and Decomposition Identity. Let S_{AM_i} denote the sequence corresponding to the template labeled AM_i, and let R be the input tandem repeat sequence. The reconstructed sequence RS is denoted as $S_{AM_1} \circ S_{AM_2} \circ \cdots \circ S_{AM_{AN}}$, where the symbol "$\circ$" represents the concatenation operation. The edit distance between RS and R is defined as the Decomposition Distance:

$$\text{Decomposition Distance} = EditDistance(R, RS) \tag{3}$$

Correspondingly, the identity between RS and R is then defined as the Decomposition Identity:

$$\text{Decomposition Identity} = 1 - \frac{EditDistance(R, RS)}{Length(R)} \tag{4}$$

WSD outperforms SD on simulated datasets

We first compared WSD and SD on simulated assembly datasets, and the specific results are shown in Figure 2. Whether the string decomposition is based on monomers or HORs, WSD demonstrates clear advantages in both speed and memory usage, speedup greater than 4.4 and usage ratio greater than 51.5 (see Figure 2A, B). WSD can complete the decomposition of a dataset in 0.08s to 15.81s, requiring only 20MB to 126MB of memory, whereas SD takes 4.3s to 29.89s and requires 1558MB to 6182MB of memory. Exact values can be found in Supplemental Table S3 and S4. Specifically, when decomposing sequences based on monomers, WSD is up to 17 times faster than SD, using only 1/40

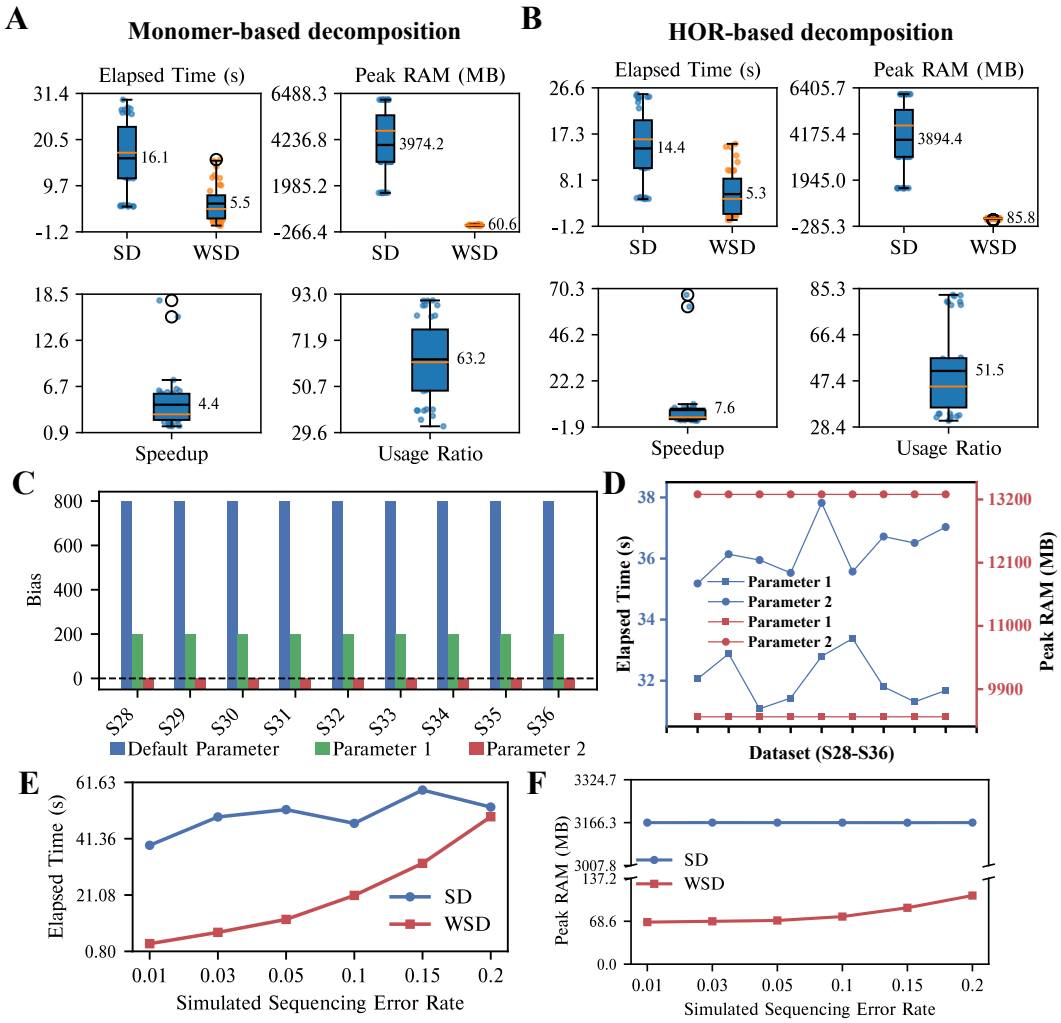

Figure 2: **Evaluation of the two methods on simulated datasets. A.** Runtime and peak memory usage for the decomposition of R1-R36 using monomers as templates, along with the speedup and usage ratio of WSD. **B.** Runtime and peak memory usage for the decomposition of R1–R36 using a HOR as a template, along with the speedup and usage ratio of WSD. **C.** Bias of SD with three different parameter settings using a HOR as a template. Parameter 1: *stringDecomposer -b 7500 -v 1000*. Parameter 2: *stringDecomposer -b 10000 -v 2000* **D.** Running time and memory usage of SD with two different parameters. **E.** Runtime of all methods on datasets (SR19-SR24) with different sequencing error rates. **F.** Peak memory usage of all methods on datasets (SR19-SR24) with different sequencing error rates.

of the memory. When decomposing sequences based on HORs, WSD is up to 53 times faster, requiring only 1/82 of the memory of SD.

Additionally, Supplemental Table S5 shows that when decomposing sequences based on monomers, both methods achieves perfect decomposition results across datasets S1-S36. However, when decomposing sequences based on HORs, SD shows significant bias on datasets S10-S36, WSD still achieves perfect decomposition results (see Supplemental Table S6).

We observe that SD has lower decomposition accuracy and higher bias on datasets with longer templates. To address this, we re-ran SD on datasets S28-S36 with two different parameter settings, and obtained new results. As

shown in Figure 2C, compared to the results using the default parameters, SD's bias significantly reduced under parameters 1 and 2, with parameter 2 achieving a bias of 0 (accuracy is also 100%). These parameters determine how the TR is divided into subsequences, and different divisions yield varying decomposition accuracies. Although SD also achieved the perfect decomposition result with parameter 2, it also led to longer running times and increased memory usage (Figure 2D). In contrast, WSD adopts a simple strategy that adaptively decides a subsequence division based on template length (see **Methods**), ensuring the robust decomposition results.

The performance of WSD depends on the divergence between the template and the target tandem repeat sequences (see **Methods**). To assess this, we evaluated WSD and SD on simulated sequencing datasets (SR1–SR24) generated with different error rates, where higher error rates indicate greater divergence between the template and the sequences. Error rates of 0.01, 0.03, and 0.05 represent typical modern sequencing conditions, whereas error rates of 0.10, 0.15, and 0.20 represent low-quality sequencing. Across all datasets SR1–SR24, both WSD and SD consistently produced correct decompositions (Supplemental Table S7 and S8). In terms of computational efficiency and memory usage, WSD showed a clear advantage. For example, at an error rate of 0.01 with a read length of 5,000 bp (SR1), WSD completed the decomposition of SR1 in 2 s, which was about 30 times faster than SD, while using only one fifty-ninth of the memory used by SD. With a read length of 20,000 bp, WSD remained about 10 times faster than SD and used only one forty-seventh of the memory. Detailed results can be found in Supplemental Table S9 and S10. As the read length increased to 20,000 bp and the error rate became higher, the performance difference between WSD and SD gradually decreased (Figure 2E). When the sequencing error rate reached 0.20, WSD and SD showed similar runtime performance; however, WSD continued to show a clear memory advantage (Figure 2F).

WSD outperforms SD on real-world datasets

We compared WSD and SD on human centromeric assemblies and Arabidopsis centromeric assemblies. In terms of decomposition results, WSD and SD produced nearly identical outputs, with small differences in the number of decomposed blocks, decomposition distance, and the decomposition identity. Exact values can be found in Supplemental Table S11, S12, Table 1, and Table 2.

WSD demonstrates significant advantages in both speed and memory usage. As shown in Table 1 and 2, WSD outperforms SD in decomposition speed for the majority of centromeres, with only a few cases where it is slightly

slower. Notably, all of these slower cases share a common feature: they contain extremely long high-divergence regions exceeding 4,400 bp (see Supplemental Figure S1). Compared to human centromeres, both methods can decompose Arabidopsis centromeres more efficiently due to their shorter length and significantly lower number of monomers. Notably, when decomposing the centromere of human Chromosome 13, SD takes 362.69 seconds, whereas WSD completes the task in just 77.61 seconds—a 4.67-fold speedup. On average, WSD is 2.33 times faster across human centromeres.

Table 1: Performance of the two methods on human centromeric assemblies using 36 threads. SD uses the default parameters, while WSD uses the parameter *"-A1"* with all other parameters set to their default values.

Chromosome	Elapsed Time (s)		Speedup	Peak RAM (MB)		Usage Ratio	Decomposition Identity	
	SD	WSD		SD	WSD		SD	WSD
1	500.26	237.03	2.11	138271.14	2379.06	58.12	0.9878	0.9879
2	370.17	281.42	1.32	138263.84	1774.79	77.90	0.9801	0.9801
3	307.10	98.37	3.12	138259.23	412.61	335.09	0.9924	0.9924
4	283.96	102.70	2.76	138258.62	269.03	513.92	0.9905	0.9905
5	395.54	203.87	1.94	138264.43	1353.27	102.17	0.9869	0.9869
6	412.96	89.49	4.61	138265.18	1651.03	83.74	0.9963	0.9963
7	391.33	150.76	2.60	138266.92	1703.16	81.18	0.9936	0.9936
8	349.36	400.03	0.87	138263.24	1586.27	87.16	0.9912	0.9912
9	355.95	162.37	2.19	138264.88	1261.57	109.60	0.9854	0.9854
10	355.01	152.76	2.32	138263.00	907.48	152.36	0.9875	0.9875
11	434.39	137.02	3.17	138267.09	1700.92	81.29	0.9866	0.9866
12	391.67	191.91	2.04	138265.51	1228.88	112.51	0.9877	0.9877
13	362.69	77.61	4.67	138262.50	1022.98	135.16	0.9949	0.9949
14	377.61	111.55	3.39	138265.47	1469.97	94.06	0.9903	0.9902
15	293.88	115.67	2.54	138259.65	500.17	276.42	0.9908	0.9908
16	363.92	373.82	0.97	138262.79	964.52	143.35	0.9889	0.9889
17	448.27	505.54	0.89	138268.64	1806.00	76.56	0.9921	0.9920
18	476.73	220.09	2.17	138271.41	2470.22	55.98	0.9885	0.9885
19	450.41	215.36	2.09	138268.91	2147.89	64.37	0.9833	0.9833
20	367.74	116.95	3.14	138263.62	980.42	141.02	0.9909	0.9909
21	251.38	154.96	1.62	134888.57	161.95	832.93	0.9859	0.9860
22	421.47	173.22	2.43	138266.49	1211.66	114.11	0.9902	0.9902
X	440.30	531.44	0.83	138266.33	1712.48	80.74	0.9894	0.9893

Table 2: Performance of the two methods on Arabidopsis centromeric assemblies using 36 threads. SD uses the default parameters, while WSD uses the parameter *"-A1"* with all other parameters set to their default values.

Chromosome	Elapsed Time (s)		Speedup	Peak RAM (MB)		Usage Ratio	Decomposition Identity	
	SD	WSD		SD	WSD		SD	WSD
1	14.97	10.41	1.44	5593.40	35.07	159.51	0.9682	0.9681
2	12.52	7.97	1.57	5592.08	32.54	171.86	0.9649	0.9650
3	11.60	7.47	1.55	5591.11	29.01	192.75	0.9585	0.9586
4	12.89	9.68	1.33	5592.02	34.76	160.89	0.9547	0.9548
5	9.86	10.99	0.90	5590.27	22.68	246.49	0.9524	0.9521

In addition to speed, WSD also has a substantial memory advantage. When processing human centromeres, SD requires at least 138,300 MB of memory, whereas WSD needs only 2,500 MB. On average, WSD's memory consumption is only 1/165 that of SD. Similarly, when analyzing Arabidopsis centromeres, WSD maintains its memory efficiency, requiring only 40 MB, while SD needs at least 5,594 MB. On average, WSD uses just 1/186 of the memory required by SD.

Discussion

In this study, we developed a novel sequence decomposition algorithm called WSD to enable more accurate, stable, and efficient TRs analysis. By leveraging the wavefront technique, WSD significantly reduces the computational and memory costs associated with sequence decomposition. Additionally, the incorporation of two adaptive sequence partitioning/pruning strategies mitigates parameter sensitivity and further enhances computational efficiency. Simultaneously, restricting penalties to integers simplifies dynamic programming and ensures numerical stability without compromising qualitative behavior. Collectively, this optimized efficiency unlocks the potential for population-level studies of alpha satellite regions, which involves processing thousands of genomes. Furthermore, our method facilitates the integration of these complex regions into pangenome graphs, a task that requires both accuracy and computational efficiency.

Although extensive tests show that WSD efficiently decomposes both TR assemblies and long reads, its computational performance is influenced by the divergence between the input sequence and the template set. When the divergence becomes large (for example, above 20%), the speed advantage of the algorithm may decrease. In practical situations, regions with high divergence, such as pericentromeric segments, leads to slower computation. These findings indicate that WSD is most effective when it is applied to genomic regions that have moderate or high similarity to the templates.

Based on these characteristics, several directions may help further improve WSD. One possible direction is to add preprocessing modules that detect regions that do not contain tandem repeats or regions that show weak similarity to the template set. Limiting WSD to intervals with strong similarity would allow the algorithm to maintain its computational advantages and reduce unnecessary processing in low-similarity regions. Building on this idea, a hybrid framework that estimates local divergence and selectively applies either WSD or a standard alignment-based method could further

improve efficiency while preserving the advantages of WSD in regions where repeat structure is well maintained. In addition, incorporating automatic identification of tandem array boundaries would improve usability and facilitate large-scale analyses, representing an important direction for future development.

Memory usage is another area where WSD may be improved. Incorporating ideas from biWFA (Marco-Sola et al., 2023) may help WSD reduce complexity. In addition, the current implementation uses a linear-gap scoring model for the sake of efficiency. Adding support for an affine-gap scoring model would allow WSD to better handle cases that involve structural insertions, such as retrotransposons. Conceptually, extending WSD to affine-gap scoring is possible, but it requires modifying the dynamic-programming formulation. In particular, each block alignment would need to maintain three wavefront states, match or mismatch (M), insertion (I), and deletion (D), as in the classical affine-gap model (Gotoh, 1982). In a wavefront framework, this means that three related wavefronts must be computed along each diagonal, with each wavefront following its own recurrence and extension rules. The template-transition mechanism would also need to propagate these states correctly across template boundaries, whereas the extension procedure would continue to operate only on the M state.

It is important to note that the completeness of sequence decomposition depends on the completeness of the input monomer library. This is a general property of methods that rely on predefined monomer sets, including WSD and StringDecomposer. When real centromeres contain highly divergent monomers or novel variants that are not represented in the input library, sequence similarity decreases and these regions may not be included in the reconstructed sequence. As a result, aligning the reconstructed sequence back to the genome can reveal large gaps, often with lengths that are multiples of the monomer size, corresponding to these unrepresented variants. Therefore, improving and expanding the monomer library to better capture centromere sequence diversity is an important direction for reducing such gaps in future analyses.

Methods

String decomposition problem

Let $R = r_1 r_2 \dots r_n$ be a tandem repeat sequence, and let $M_1, M_2, \dots, M_t$ be a series of template sequences, where $M_j = m_{j1} m_{j2} \dots m_{jl_j}$. Let block B_α be a subsequence of R, and let interval(B_α) denote the coordinate interval—consisting of the start and end positions of B_α on R. Then, the string decomposition problem can be formulated as the following

optimization problem:

$$\begin{aligned} &\min_{1\le x\le n} \sum_{\alpha=1}^{x} cost(B_\alpha, M_{\beta_x}),\ \beta_x \in \{1,2,..,t\} \\ \text{s.t.}\quad &\begin{cases} B_1 \circ B_2 ... \circ B_x = R. \\ \forall 1 \le \gamma, \delta \le x,\ \gamma \ne \delta, interval(B_\gamma) \cap interval(B_\delta) = \emptyset. \end{cases} \end{aligned} \tag{5}$$

Here, the function $cost(*)$ represents the cost of aligning two strings. Next, we demonstrate how to solve the above optimization problem based on the WSD algorithm.

A sequence-alignment-like DP solution

SD introduces the construction of a String Decomposition graph (SD graph), where the longest (heaviest) path in the graph represents the optimal solution to the string decomposition problem (Dvorkina et al., 2020). In fact, the heaviest path in the SD graph corresponds directly to the optimal solution of Equation (5). If the decomposition represented by a path in the SD graph consists of x blocks, then the path contains $x - 1$ "block-switching" edges (each with weight 0). The total weight of this path is therefore the sum of the weights contributed by the x alignment graphs associated with these blocks. Note that, although the edge weights in the SD graph are formulated so that a larger weight corresponds to a better (i.e., lower-cost) block alignment, the weight assigned to each block is exactly a monotonic transformation of the cost defined in Equation (5). Consequently, maximizing the path weight in the SD graph is equivalent to minimizing the total cost in Equation (5). Hence, the optimization problem in Equation (5) is mathematically equivalent to finding the heaviest path in the SD graph.

String decomposition can be formulated as a DP problem analogous to sequence alignment. Specifically, assume that the penalty score for a mismatch is h and the penalty score for a gap is g, where both h and g are strictly greater than 0. When character y is not equal to z, the penalty function is defined as $s(y, z) = h$; otherwise, it is 0. We define a three-dimensional DP matrix D, where i, j, k are the indices corresponding to the input sequence R, the template set, and the template sequence within the set, respectively. The cell $D[i][j][k]$ represents the optimal decomposition cost of the prefix subsequence $R' = r_1 r_2 \dots r_i$ $(i \le n)$ under the specific condition that the decomposition ends with the block corresponding to the subsequence $m_{j1} m_{j2} \dots m_{jk}$ of the j-th template. Thus, each entry $D[i][j][k]$ encodes the best cost among all decompositions of R' that terminate in this particular template–state configuration. To obtain

the overall optimal decomposition cost of R', we take the minimum over all templates j and valid template positions k:

$$Cost_i = \min_{1 \le i \le n,\ 1 \le j \le t,\ 1 \le k \le l_j} D[i][j][k]. \tag{6}$$

where t is the number of templates and l_j represents the length of jth template. Similar to sequence alignment, when $i = 1$ and $k = 1$, for all j, we have $D[1][j][1] = s(r_1, m_{j1})$. When $i = 1$ and $k > 1$, we have:

$$D[1][j][k] = \min\left((k-1) \cdot g + s(r_1, m_{jk}),\ D[1][j][k-1] + g\right). \tag{7}$$

When $i > 1$, we have the following recurrence relation:

$$D[i][j][k] = min \begin{cases} D[i-1][j][k-1] + s(r_i, m_{jk}), & (k > 1) \\ D[i][j][k-1] + g, & (k > 1) \\ D[i-1][j][k] + g, & (k \ge 1) \\ \min\limits_{1 \le j_* \le t} D[i-1][j_*][l_{j_*}] + s(r_i, m_{jk}) & (k = 1) \end{cases} \tag{8}$$

We can regard D as t sequence-alignment DP matrices corresponding to R and each M_j. Unlike a standard sequence-alignment DP matrix, when $k = 1$, $D[i][j][k]$ depends not only on its left neighbor $D[i-1][j][k]$ but also on all $D[i-1][j_*][l_{j_*}]_{1 \le j_* \le t}$. This additional dependency reveals a template-transition in the string decomposition problem—namely, once the sequence alignment reaches the last character of a particular template, the subsequent alignment step may jump to the first character of another template.

Once D is computed, similar to sequence alignment, we start backtracking from a cell with cost $\min\limits_{1 \le j \le t,\ 1 \le k \le l_j} D[n][j][k]$ in D until reaching another cell $D[1][j][1], 1 \le j \le t$. The backtracking path records the decomposition result of R. The computational complexity and space complexity of this DP scheme are both $O(n \cdot \sum_{j=1}^{t} l_j)$. Although this DP approach is elegant, its runtime and memory consumption increase significantly when R is long and the template set is large. The WSD algorithm introduces a novel DP strategy that eliminates the need to compute and store many DP cells while still obtaining the decomposition results. Details are provided below.

WSD algorithm: a wavefront-based DP solution

Figure 3A-C shows a computational example of WSD. "Wavefront" is essentially a set of cells in the DP matrix that satisfy certain conditions (Marco-Sola et al., 2021). Specifically, we consider the matrix D and a specific cell (i, j, k) within it, where i and k correspond to the indices of the reference sequence R and the template sequence

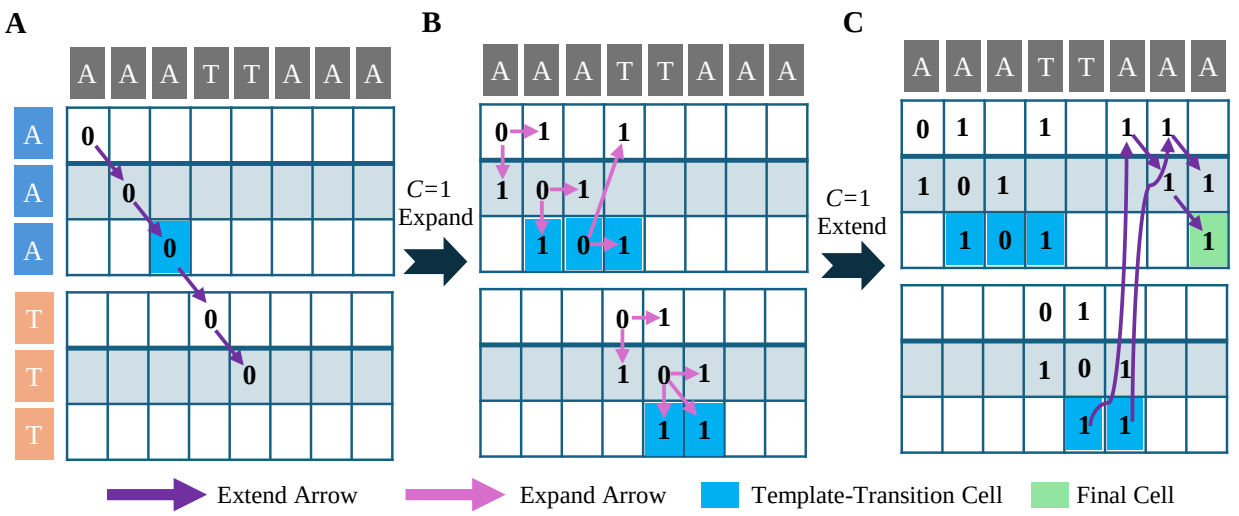

Figure 3: **A computational example of WSD (with mismatch and gap penalties set to 1 in this example).** Arrows of different colors indicate the origin of the cell. **A.** When the cost score $c = 0$, the extend function is executed. **B.** When $c = 0$ and the final cell cannot be reached, the cost score c is incremented and the expand function is executed. **C.** When the cost score $c = 1$, the extend function is executed.

M_j, respectively, we define the position of this cell in the sequence alignment-like DP matrix for the jth template. Specifically, we denote this position in a diagonal with index d, where $d = i - k$, and represent this diagonal as an ordered pair (j, d).

Given a cost score c, we define $F_{c,j,d}$ as the farthest cell along the diagonal (j, d) that maintains a cost score of c. The reference index of $F_{c,j,d}$, referred to as the *offset*, is denoted by $W_{c,j,d}$. A cell Cell_x is considered farther than a cell Cell_y along the same diagonal if its *offset* is greater than that of Cell_y. We define a function ETP (**E**xtending **T**he **P**refix):

$$ETP(W, R, M) := W + LCP(R[W + 1 :], M[W + 1 - d :]) \tag{9}$$

Similar to Equation (8), the recursive relation for $W_{c,j,d}$ can be derived as follows:

$$W_{c,j,d} = max \begin{cases} ETP(W_{c-h,j,d} + 1, R, M_j), \\ ETP(W_{c-g,j,d+1}, R, M_j), \\ ETP(W_{c-g,j,d-1} + 1, R, M_j), \\ ETP(d + 1, R, M_j) \quad (\text{if } \exists j' \ (1 \le j' \le t),\ s.t.\ W_{c-h,j',d-l_{j'}} = d \ \&\& \ d \ge 0\ ) \end{cases} \tag{10}$$

Here, LCP$(*, *)$ denotes the length of the longest common prefix between two strings, and the notation $[:]$ represents the slicing operation. For example, given an integer p_x $(1 \le p_x \le n)$, $R[p_x :]$ represents the subsequence $r_{p_x} r_{p_x+1} \ldots r_n$. Initially, for each j, if $r_1 = m_{j1}$ the variable $W_{0,j,0}$ is initialized to 1; otherwise, it is initialized to 0. Supplemental Figure S2 further visualizes the dependencies of Equation (10).

Algorithm 1: WSD algorithm

input : Reference sequence $R = r_1 r_2 ... r_n$, template set $T \leftarrow \{M_1, M_2, ..., M_t\}$, gap/mismatch penalty score g/h

output String decomposition result $\widetilde{D}$

:

$c \leftarrow 0$; $offset \leftarrow 0$; $W_{0,j,0} \leftarrow 1$ (if $r_1 = m_{j1}$) or 0 (otherwise) ▷ Initial conditions

while *true* **do**

  extend$(R, T, W, offset, c)$ ▷ Calculate Part 1

  if $offset \geq n$ **then**

    break ▷ Decomposition is finished

  $c \leftarrow c + 1$

  expand(W, c) ▷ Calculate Part 2

$\widetilde{D} \leftarrow$ Backtrace(W, c, g, h, R, T)

return $\widetilde{D}$

The WSD algorithm is centered around Equation (10) (see Algorithm 1). To facilitate understanding, each recurrence relation in Equation (10) can be divided into two components: the first component is the LCP function (referred to as Part 1), and the second consists of the remaining terms in the equation (referred to as Part 2). Part 1 is computed using the extend function (see Algorithm 2), while Part 2 is handled by the expand function (see Algorithm 3). There is a subtle but important detail here. Algorithm 3 suggests that we first determine the maximum among $W_{c-h,j,d} + 1$, $W_{c-g,j,d+1}$, and $W_{c-g,j,d-1} + 1$, and then perform the extend procedure starting from this maximum value. In contrast, Equation (10) implies that the extend procedure should be executed starting from all three values $W_{c-h,j,d} + 1$, $W_{c-g,j,d+1}$, and $W_{c-g,j,d-1} + 1$, followed by taking the maximum of their extension results. We claim that these two approaches are equivalent; that is: $ETP(max(a, b),\ R,\ M) = max(ETP(a,\ R,\ M), ETP(b,\ R,\ M))$. The details of the proof are in Supplementary Note 3.

The extend function iteratively verifies whether characters at corresponding positions along each diagonal are identical. When a mismatch occurs, it signifies that the farthest point under the current cost c has been reached. If the $offset$ at this point remains less than n, it indicates that the minimum decomposition cost of R exceeds c. In this case, c is incremented, and the expand function is executed. The expand function initializes a new wavefront for selected diagonals under the updated cost $c + 1$. The extend function then utilizes this newly established wavefront to continue extending the diagonals until their respective farthest points are reached. Notably, the extend function consists of two steps. First, it operates within the DP matrix of the corresponding template (Algorithm 2, line 11-18), adding all template-transition cells to a queue q. Then, the extension proceeds based on q (Algorithm 2, lines 19–30): Although the current alignment may reach the end of a block on a particular template, the match does not necessarily terminate at

Algorithm 2: Extend function

input : Reference sequence $R = r_1 r_2 ... r_n$, template set $T \leftarrow \{M_1, M_2, ..., M_t\}$, Wavefront W, offset $offset$, cost score c

Function `ExtendDiagonal`$(W, offset, u, v, j, d)$**:**
- **while** $r_u == m_{jv}$ **do**
  - $W_{c,j,d} \leftarrow W_{c,j,d} + 1$
  - $u \leftarrow u + 1$
  - $v \leftarrow v + 1$
- **if** $W_{c,j,d} == \min(v + l_j, n)$ **then**
  - $q.push([j, d])$ ▷ Obtain a template-transition cell
- $offset = \max(offset, W_{c,j,d})$
- **if** $offset \geq n$ **then**
  - **return**

Function `Extend`$(R, T, W, offset, c)$**:**
- $q \leftarrow queue()$ ▷ A FIFO queue to store template-transition cells
- **for** $1 \leftarrow j$ *to* t **do**
  - **for** $1 - l_j \leftarrow d$ *to* $n - 1$ **do**
    - **if** $W_{c,j,d} \neq 0$ **then**
      - $u \leftarrow W_{c,j,d} + 1$
      - $v \leftarrow W_{c,j,d} - d + 1$
      - `ExtendDiagonal`$(W, offset, u, v, j, d)$
- **while** q *not empty* **do**
  - $[x, y] \leftarrow q.pop()$
  - $p_r \leftarrow W_{c,x,y}$
  - **for** $1 \leftarrow j$ *to* t **do**
    - **if** $r_{p_r+1} == m_{j1}$ **then**
      - $W_{c,j,p_r} \leftarrow p_r + 1$
      - $u \leftarrow W_{c,j,p_r} + 1$
      - $v \leftarrow 2$
      - `ExtendDiagonal`$(W, offset, u, v, j, p_r)$
    - **else**
      - **if** $W_{c+h,j,p_r} == 0$ **then**
        - $W_{c+h,j,p_r} \leftarrow p_r + 1$ ▷ This suggests a mismatch so expand W_{c,j,p_r} to obtain W_{c+h,j,p_r}

this cell. It is still possible to continue extending the decomposition by switching to other templates. When the $offset$ is greater than or equal to n, backtracking process is used to obtain the final decomposition result. The backtracking scheme is similar to that used in sequence alignment.

Algorithm 3: Expand function

input : Wavefront W, cost score c, gap/mismatch penalty score g/h

Function `Expand`(W, c)**:**
- **for** $1 \leftarrow j$ *to* t **do**
  - **for** $1 - l_j \leftarrow d$ *to* $n - 1$ **do**
    - $W_{c,j,d} = \max\left\{W_{c-h,j,d} + 1, W_{c-g,j,d+1}, W_{c-g,j,d-1} + 1\right\}$

Runtime complexity and memory footprint

We assume that the tandem repeat sequence has length n, and that t templates are provided, each of length at most n.

Let c denote the total decomposition cost. Under these assumptions, the theoretical time complexity of WSD is $O(tnc)$ and the space complexity is $O(tc^2)$.

In WSD, the t templates correspond to t DP matrices. For a single DP matrix, the expand procedure activates $O(c)$ diagonals, each of which triggers an extend operation. Since each extend operation performs $O(n)$ work, the computation per DP matrix is bounded by $O(nc)$. As shown in Algorithm 1, WSD performs $O(c)$ iterations. If the cost at iteration i is s ($0 \leq s \leq c$), then $O(s)$ diagonals contain offsets that must be stored. Summed over all iterations, the total number of stored offsets is bounded by $\sum_{s=0}^{c} O(s) = O(c^2)$. Considering all t DP matrices, the overall time and space complexities are therefore $O(tnc)$ and $O(tc^2)$, respectively.

Empirical evaluation on simulated datasets supports this analysis: the running time of WSD scales approximately linearly with both c and t, while memory usage grows linearly with t (Figure 2E, Supplemental Figure S3). The theoretically expected quadratic dependence on c in memory usage was not prominent in practice. Similar behavior was also observed for the WFA algorithm (Marco-Sola et al., 2021).

WSD algorithm: two adaptive strategies

We employ two strategies to accelerate the WSD algorithm. The first strategy leverages a simple yet highly effective adaptive approach to partition long tandem repeat sequences into shorter subsequences. The decomposition results of these subsequences are then integrated to obtain the final decomposition of the long tandem repeat sequences. This approach eliminates the need for user-defined hyperparameters while ensuring decomposition accuracy (see **Results**). Specifically, we determine the subsequence length based on the input template length. Given a maximum template sequence length L, the subsequence length is set to $2L$. Since sequence partitioning primarily affects the last block of each subsequence decomposition, the starting position of the next subsequence in the long tandem sequence is aligned with the starting point of the last block in the previous subsequence. Additionally, the WSD algorithm incorporates a parallelization scheme for ultra-long tandem repeat assemblies. These long sequences are divided into subsequences of length $1000L$ with an overlap of $10L$. Each subsequence can be decomposed in parallel, and their results are then integrated to obtain the final decomposition.

The second strategy involves pruning the WSD algorithm itself. As the cost score increases, the wavefront set in WSD expands, leading to a growing number of diagonals that require calculation via the extend and expand functions.

During iterations, the algorithm tracks the maximum offset. When the cost score reaches a predefined threshold (default: 10), if the difference between the current diagonal's offset and the maximum offset exceeds a predefined limit (default: 100), the diagonal is deemed unlikely to be part of the optimal path. The default parameters were chosen empirically during tool development. Although not based on a comprehensive parameter search, large-scale simulations confirmed that these settings are robust across a wide range of sequence lengths, repeat architectures, and mutation rates. Further details on all parameters are provided in Supplementary Note 4.

To further quantify the contributions of the two adaptive strategies, we performed an ablation study. The results show that both strategies accelerate the WSD algorithm and maintain accurate decomposition results, with the first adaptive strategy providing the most substantial improvement (see Supplemental Table S13–S15). Specifically, compared with the version without any adaptive strategies, using only the first adaptive resulted in an approximately 400-fold speedup while reducing memory usage to about $1/100$ of the original. Using only the second adaptive strategy produced a more modest performance gain of about 1.5-fold and reduced memory usage to roughly one quarter of the original.

Code availability

The source code of WSD is available at `https://github.com/junhaiqi/wsd` under the MIT License and as Supplemental Code. All benchmarking data and scripts required to reproduce this work are available at Figshare (`https://doi.org/10.6084/m9.figshare.30818273`) and as Supplemental Data.

Acknowledgements

This work was supported by the National Key R&D Program of China with code 2020YFA0712400, the National Natural Science Foundation of China with code 12471461, and the Fundamental Research Funds for the Central Universities. The funders had no role in study design, data collection and analysis, decision to publish, or preparation of the manuscript.

Author contributions

J.Q. conceived and developed WSD. J.Q. conducted the benchmarking analyses and contributed to data analysis alongside T.Y.. J.Q. drafted the manuscript, which was subsequently revised by T.Y., Z.Y.. All authors reviewed and

approved the final version of the manuscript. G.L. and T.Y. supervised and coordinated the project.

Competing interests

The authors declare that they have no competing interests.

References

Bahk K and Sung J. 2024. Sigalign: an alignment algorithm guided by explicit similarity criteria. *Nucleic Acids Research* **52**: 8717–8733.

Benson G. 1999. Tandem repeats finder: a program to analyze dna sequences. *Nucleic Acids Research* **27**: 573–580.

Bzikadze AV and Pevzner PA. 2020. Automated assembly of centromeres from ultra-long error-prone reads. *Nature Biotechnology* **38**: 1309–1316.

Depienne C and Mandel JL. 2021. 30 years of repeat expansion disorders: What have we learned and what are the remaining challenges? *The American Journal of Human Genetics* **108**: 764–785.

Dvorkina T, Bzikadze AV, and Pevzner PA. 2020. The string decomposition problem and its applications to centromere analysis and assembly. *Bioinformatics* **36**: i93–i101.

Gao S, Yang X, Guo H, Zhao X, Wang B, and Ye K. 2023. Hicat: a tool for automatic annotation of centromere structure. *Genome Biology* **24**: 58.

Gao S, Zhang Y, Bush SJ, Wang B, Yang X, and Ye K. 2024. Centromere landscapes resolved from hundreds of human genomes. *Genomics, Proteomics & Bioinformatics* **22**: qzae071.

Gotoh O. 1982. An improved algorithm for matching biological sequences. *Journal of Molecular Biology* **162**: 705–708.

Harris RS, Cechova M, and Makova KD. 2019. Noise-cancelling repeat finder: uncovering tandem repeats in error-prone long-read sequencing data. *Bioinformatics* **35**: 4809–4811.

Ichikawa K, Kawahara R, Asano T, and Morishita S. 2023. A landscape of complex tandem repeats within individual human genomes. *Nature Communications* **14**: 5530.

Kunyavskaya O, Dvorkina T, Bzikadze AV, Alexandrov IA, and Pevzner PA. 2022. Automated annotation of human centromeres with hormon. *Genome Research* **32**: 1137–1151.

Li H and Durbin R. 2024. Genome assembly in the telomere-to-telomere era. *Nature Reviews Genetics* **25**: 658–670.

Logsdon GA, Rozanski AN, Ryabov F, Potapova T, Shepelev VA, Catacchio CR, Porubsky D, Mao Y, Yoo D, Rautiainen M, et al.. 2024. The variation and evolution of complete human centromeres. *Nature* **629**: 136–145.

Marco-Sola S, Eizenga JM, Guarracino A, Paten B, Garrison E, and Moreto M. 2023. Optimal gap-affine alignment in o(s) space. *Bioinformatics* **39**: btad074.

Marco-Sola S, Moure JC, Moreto M, and Espinosa A. 2021. Fast gap-affine pairwise alignment using the wavefront algorithm. *Bioinformatics* **37**: 456–463.

353 Masutani B, Kawahara R, and Morishita S. 2023. Decomposing mosaic tandem repeats accurately from long reads. *Bioinformatics* **39**: btad185.

354 Naish M, Alonge M, Wlodzimierz P, Tock AJ, Abramson BW, Schmücker A, Mandáková T, Jamge B, Lambing C, Kuo P, et al.. 2021. The genetic and epigenetic
355 landscape of the arabidopsis centromeres. *Science* **374**: eabi7489.

356 Needleman SB and Wunsch CD. 1970. A general method applicable to the search for similarities in the amino acid sequence of two proteins. *Journal of Molecular*
357 *Biology* **48**: 443–453.

358 Nurk S, Koren S, Rhie A, Rautiainen M, Bzikadze AV, Mikheenko A, Vollger MR, Altemose N, Uralsky L, Gershman A, et al.. 2022. The complete sequence of a human
359 genome. *Science* **376**: 44–53.

360 Park J, Kaufman E, Valdmanis PN, and Bafna V. 2023. Trviz: a python library for decomposing and visualizing tandem repeat sequences. *Bioinformatics Advances* **3**:
361 vbad058.

362 Qi J, Ma J, Han R, Han Z, Yu T, and Li G. 2025. De novo annotation of centromere with centroanno. *bioRxiv doi: 10.1101/123456* .

363 Ren J, Gu B, and Chaisson MJ. 2023. Vamos: variable-number tandem repeats annotation using efficient motif sets. *Genome Biology* **24**: 175.

364 Ting DT, Lipson D, Paul S, Brannigan BW, Akhavanfard S, Coffman EJ, Contino G, Deshpande V, Iafrate AJ, Letovsky S, et al.. 2011. Aberrant overexpression of
365 satellite repeats in pancreatic and other epithelial cancers. *Science* **331**: 593–596.

366 Zhang P, Wei Y, Tian Q, Zou Q, and Wang Y. 2025. Fast sequence alignment for centromere with rama. *Genome Research* pp. gr–279763.